



Alpha1-antitrypsin counteracts heme-induced endothelial cell inflammatory activation, autophagy dysfunction and death

Kukuh Madyaningrana^{a,g,1}, Vijith Vijayan^{a,1}, Christoph Nikolin^a, Abid Aljabri^a, Srinu Tumpara^b, Elena Korenbaum^c, Harshit Shah^d, Metodi Stankov^e, Heiko Fuchs^f, Sabina Janciauskiene^b, Stephan Immenschuh^{a,*}

^a Institute of Transfusion Medicine and Transplant Engineering, Hannover Medical School, Hannover, Germany

^b Department of Pulmonology, Biomedical Research in Endstage and Obstructive Lung Disease Hannover (BREATH), Member of the German Center for Lung Research (DZL), Hannover Medical School, Hannover, Germany

^c Institute for Biophysical Chemistry Hannover Medical School, Hannover, Germany

^d Institute for Pathology, Hannover Medical School, Hannover, Germany

^e Department for Clinical Immunology and Rheumatology, Hannover Medical School, Hannover, Germany

^f Institute of Experimental Ophthalmology, Hannover Medical School, Hannover, Germany

^g Faculty of Biotechnology, Universitas Kristen Duta Wacana, Yogyakarta, Indonesia

ARTICLE INFO

Keywords:

alpha1-antitrypsin
Endothelial cell
Cell death
Heme
Heme-binding proteins
Inflammation
Lysosome

ABSTRACT

Free heme toxicity in the vascular endothelium is critical for the pathogenesis of hemolytic disorders including sickle cell disease. In the current study, it is demonstrated that human alpha1-antitrypsin (A1AT), a serine protease inhibitor with high binding-affinity for heme, rescues endothelial cell (EC) injury caused by free heme. A1AT provided endothelial protection against free heme toxicity via a pathway that differs from human serum albumin and hemopexin, two prototypical heme-binding proteins. A1AT inhibited heme-mediated pro-inflammatory activation and death of ECs, but did not affect the increase in intracellular heme levels and up-regulation of the heme-inducible enzyme heme oxygenase-1. Moreover, A1AT reduced heme-mediated generation of mitochondrial reactive oxygen species. Extracellular free heme led to an increased up-take of A1AT by ECs, which was detected in lysosomes and was found to reduce heme-dependent alkalization of these organelles. Finally, A1AT was able to restore heme-dependent dysfunctional autophagy in ECs. Taken together, our findings show that A1AT rescues ECs from free heme-mediated pro-inflammatory activation, cell death and dysfunctional autophagy. Hence, A1AT therapy may be useful in the treatment of hemolytic disorders such as sickle cell disease.

1. Introduction

The vascular endothelium plays a major role in regulating the homeostasis of blood pressure, the plasma coagulation system, exchange of fluid and macromolecules between blood vessels and tissues as well as quiescence of inflammation [1–3]. In conditions associated with hemolysis and tissue damage such as sickle cell disease or ischemia-reperfusion injury (IRI) the endothelium encounters high levels of free heme released from damaged red blood cells or tissues [4–6]. Free heme can have pro-oxidant, pro-inflammatory and cytotoxic

effects in the endothelium if its toxicity is not contained by covalent or non-covalent binding to hemoproteins or heme-binding proteins (HBPs) [7–12]. Therefore, intra- and extracellular levels of free heme are tightly controlled via a complex interplay of various protective mechanisms. For example, intracellular levels of heme are determined through a fine-tuned balance of enzymatic heme synthesis and degradation. Moreover, complex interactions of heme with intra- and extracellular HBPs are critically involved in controlling heme homeostasis [13–17].

A prototypical serum HBP is hemopexin, a glycoprotein with high binding affinity for free heme ($K_D < 10^{-12}$ in humans) that has been

* Corresponding author. Institute for Transfusion Medicine and Transplant Engineering, Hannover Medical School, Carl-Neuberg-Str. 1, 30625, Hannover, Germany.

E-mail address: immenschuh.stephan@mh-hannover.de (S. Immenschuh).

¹ Equal contribution.

shown to counter-act free heme toxicity [18–20]. In conditions of major hemolysis serum levels of hemopexin are diminished [21] and, therefore, other serum HBP such as albumin may become essential in neutralizing free heme toxicity [9]. Although albumin binds heme with lower affinity than hemopexin, its high serum concentrations may compensate a potential deficiency in hemopexin [22]. The latter may at least partially explain protective effects of albumin infusion to individuals with severe sepsis [23] or malaria [24,25].

Human alpha1-antitrypsin (A1AT), an acute-phase glycoprotein and important inhibitor of neutrophil proteases, has been shown to exhibit relatively high heme-binding affinity similar to that of albumin ($K_D \sim 10^{-7}$ in humans) [26]. We have previously reported in a human neutrophil model that A1AT markedly reduced free heme-activating effects such as reactive oxygen species (ROS) production, induction of heme oxygenase (HO)-1, release of interleukin (IL)-8, and inhibited neutrophil adhesion to ECs. In a mouse model of heme-induced acute kidney injury, A1AT was able to lower serum levels of heme and concomitant pro-inflammatory effects [27]. The aim of the current study was to investigate how A1AT controls heme toxicity in human ECs and to compare A1AT effects with two serum HBPs, hemopexin and albumin.

2. Results

2.1. A1AT blocks heme-induced activation of ECs

Since free heme causes inflammatory activation of ECs [28], we treated HUVECs with heme (2.5 μ M) in the absence or presence of A1AT (0.5 mg/ml). For a comparison, albumin and hemopexin, two serum HBPs with high binding affinity for heme, as well as γ -globulin, a serum protein with no known binding affinity for heme, were applied under the same experimental conditions. As expected, free heme induced the EC surface expression of VCAM-1 and ICAM-1, and the secretion of cytokine IL-8 in the cell culture supernatant (Fig. 1A–C). The effects of heme were blocked by A1AT, albumin and hemopexin, but not by γ -globulin on both protein (Fig. 1A–C) and mRNA levels (Table 1). Because EC activation by heme is mediated via the NF- κ B pathway [29], we hypothesized that treatment with the I- κ B inhibitor, Bay11-7082, will block the effects of heme. As demonstrated in Table 2, BAY11-7082 and TAK-242, a small-molecule inhibitor of Toll-Like Receptor (TLR) 4, markedly inhibited heme-induced mRNA expression of VCAM-1, ICAM-1 and IL-8 (Table 2). Furthermore, Western blot analysis revealed that A1AT, albumin and hemopexin as well as BAY11-7082 and TAK-242, inhibited heme-induced phosphorylation of the NF- κ B subunit p65 (Figs. S1A–B). These results support the notion that inhibition of heme-induced EC activation involves the NF- κ B pathway.

2.2. A1AT prevents heme-caused EC death

Heme can cause EC death via apoptosis and necroptosis [30]. As determined by 3-(4, 5-dimethylthiazol-2-yl)-2,5-diphenyltetrazolium bromide (MTT) and lactate dehydrogenase (LDH) assays, prolonged exposure of ECs to heme (18 h) induced cytotoxicity, which was prevented by A1AT, albumin and hemopexin (Fig. 2A and B), but not by γ -globulin or BAY11-7082 or TAK242 (Fig. S1B). These latter findings implied that heme-induced NF- κ B activation and/or TLR4 signaling are not involved in the observed cytotoxic effects of heme (Fig. S1C). The MTT assay, which measures cellular metabolic activity, was also applied for determining cell viability/cytotoxicity, but the results were in line with LDH assays (not shown). To further explore the mechanism/s of heme-induced cytotoxicity in ECs various small molecule inhibitors of cell death were employed. The apoptosis inhibitor Z-VAD-fmk, the necroptosis inhibitor necrostatin-1, but not the necrosis inhibitor IM-54 or the ferroptosis inhibitor ferrostatin-1, attenuated heme-induced cytotoxicity (Fig. 2C). Caspase activity assays further confirmed that treatment of ECs with heme alone, but not with heme plus A1AT, caused the activation of caspases 3 and 7 (Fig. 2D). The ability of A1AT to

abolish free heme toxicity was also observed in aortic, pulmonary microvascular, and dermal microvascular ECs (Fig. S2). Altogether, the findings show that A1AT inhibits heme-mediated EC death.

2.3. Protective effects of A1AT are independent of HO-1

Albumin and hemopexin can prevent heme toxicity via limiting its entry into ECs [31]. To explore the mechanism of A1AT-mediated EC protection we treated cells with heme or heme-A1AT and intracellular levels of labile heme were determined with an apo-horseradish peroxidase (HRP)-based assay. In contrast to albumin and hemopexin, A1AT did not block the up-take of heme by ECs (Fig. 3A) and the up-regulation of mRNA and protein levels of the inducible heme-degrading enzyme, HO-1 (Fig. 3B and C). As expected, γ -globulin showed no effect on HO-1 induction (Fig. 3C). Because the up-regulation of HO-1 gene expression is considered a cytoprotective mechanism against free heme toxicity [32], we examined whether HO-1 expression and HO activity may contribute to heme-neutralizing effects of A1AT. Hence, before adding heme alone or heme with A1AT, ECs were pretreated with the HO inhibitor tin (IV)-mesoporphyrin IX (SnMPiX). As demonstrated in Fig. 3D, pretreatment with this compound did not affect A1AT-dependent cytoprotection against heme toxicity. Similarly, a transient knock-down of HO-1 by transfection with HO-1 small interfering RNA (siRNA) (Fig. 3E) did not alter A1AT-dependent protection of ECs (Fig. 3F). Thus, A1AT cytoprotection against heme-mediated EC injury is mediated via a mechanism that differs from that of albumin and hemopexin.

2.4. A1AT blocks heme-induced mitochondrial ROS (mROS) production

Mitochondrial dysfunction is associated with apoptosis and necroptosis [33]. Therefore, we evaluated the potential role of mitochondria in heme-mediated EC death. Staining with the mROS indicator MitoSOX [34] revealed that heme-mediated up-regulation of mROS is blocked by A1AT, as similarly observed for the mitochondria-specific superoxide scavenger mito-TEMPO [35] (Fig. 4A). Among the compounds applied as positive controls for mROS, the mitochondrial respiratory chain complex III inhibitor antimycin A, but not the complex I inhibitor rotenone, induced the production of mROS (Fig. 4A). To further determine the potential role of heme toxicity via mROS, ECs were treated with heme in the presence of mito-TEMPO. Whereas mito-TEMPO significantly blocked heme-induced cell death (Fig. 4B), rotenone, carbonyl cyanide-p-trifluoromethoxyphenylhydrazone (FCCP) and oligomycin A had no or only a minor effect on heme-induced cell death (Fig. 4B). Moreover, treatment with antimycin-A, which induced mROS in this model potentiated heme-induced toxicity. These findings indicate that generation of mROS, but not inhibition of the respiratory chain, contributes to heme-mediated cell death. These data indicate that heme-dependent cytotoxicity in ECs involves an increase of mROS that is blocked by A1AT.

2.5. Intracellular levels of A1AT are increased in the presence of heme

We next asked whether A1AT-mediated cytoprotection of ECs against heme toxicity might be related to the enhanced A1AT up-take by these cells. As determined by confocal microscopy, intracellular levels of A1AT were markedly higher in cells treated with A1AT plus heme in comparison to cells treated with A1AT alone. Notably, A1AT was not detectable in untreated or heme-treated ECs (Fig. 5A). Similarly, intracellular A1AT levels increased in ECs cultured with native human plasma in the presence of heme, further confirming that heme enhances the up-take of A1AT (Fig. 5B). A1AT is known to be taken up by ECs via endocytosis that is a lysosome delivery pathway [36]. Accordingly, A1AT was found to be co-stained with LysoTracker Red indicating lysosomal localization of this protein (Fig. 5C). Altogether, the data show that free heme increases the up-take of A1AT by ECs and localizes

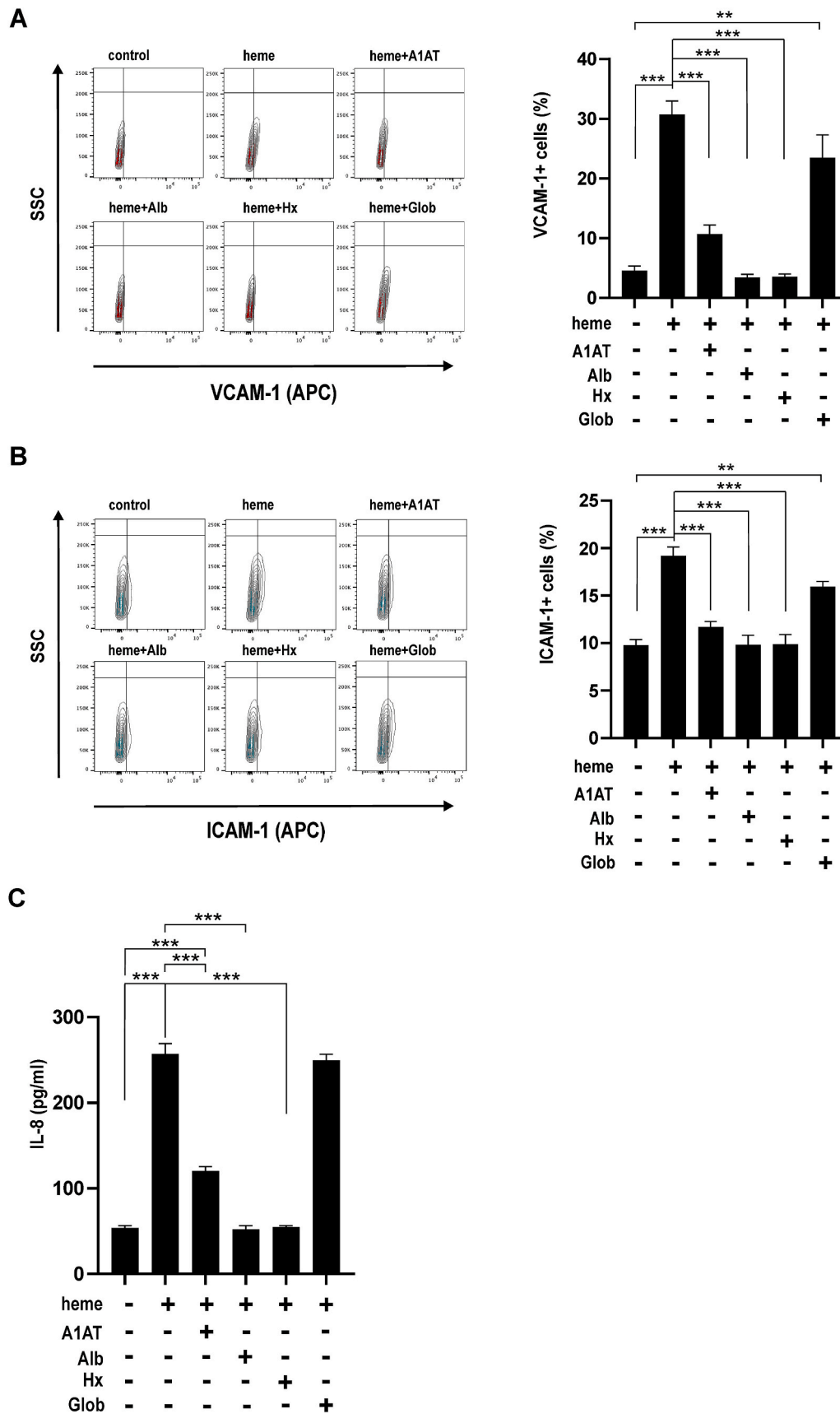


Fig. 1. A1AT attenuates heme-induced EC activation. (A–C) HUVECs were treated with heme (2.5 μ M) in the presence of A1AT (0.5 mg/ml), albumin (0.5 mg/ml), Hx (0.5 mg/ml) or γ -globulin (0.5 mg/ml) for 12 h. (A–B) The cells were probed with antibodies against VCAM-1 and ICAM-1 and analyzed by flow cytometry. A representative flow cytometry contour plot is shown (left) and the mean % positive population of VCAM-1 and ICAM-1 is represented as a bar graph. (C) The cell culture supernatant was analyzed for the levels of secreted IL-8 by ELISA. Results shown are means \pm SEM of at least three independent experiments. One-way ANOVA with Tukey’s post-hoc analysis was performed for statistical analysis, ** $p < 0.01$, *** $p < 0.001$. Alb, albumin; Hx, hemopexin; Glob, γ -globulin.

Table 1
A1AT blocks heme-induced EC activation.

Treatment	VCAM-1/HPRT	ICAM-1/HPRT	IL-8/HPRT
Control	1	1	1
A1AT	1.032 ± 0.064	1.14 ± 0.21	0.83 ± 0.34
Hx	1.46 ± 0.46	1.34 ± 0.52	1.1 ± 0.07
HSA	0.69 ± 0.14	1.24 ± 0.67	0.99 ± 0.78
Heme	20.2 ± 7.21***	29.75 ± 21.35**	67.87 ± 40.38**
Heme + A1AT	0.58 ± 0.20	1.38 ± 0.91	1.87 ± 1.66
Heme + Hx	0.46 ± 0.10	0.99 ± 0.09	1.06 ± 0.10
Heme + HSA	0.78 ± 0.12	0.91 ± 0.50	0.82 ± 0.56

HUVECs were treated with heme (2.5 μM) in the presence or absence of the indicated serum proteins (0.5 mg/ml) for 9 h. Expression of VCAM1, ICAM1 and IL-8 was analyzed by real time RT-PCR and normalized to the expression of hypoxanthine phosphoribosyltransferase 1 (HPRT). Values are represented as mean ± SD fold induction in relation to control unstimulated cells from three independent experiments. One-way ANOVA with Tukey's post-hoc analysis was performed for statistical analyses; VCAM-1 (Heme vs others ***p < 0.001), ICAM-1 (Heme vs others **p < 0.01) and IL-8 (Heme vs others **p < 0.01).

Table 2
EC activation is mediated via NF-κB and TLR4 signaling.

Treatment	VCAM-1/HPRT	ICAM-1/HPRT
Control	1	1
Bay-11082	0.59 ± 0.2	0.72 ± 0.02
TAK-242	0.87 ± 0.46	0.84 ± 0.52
Heme	15.58 ± 10.6**	49.88 ± 27.07**
Heme + Bay-11082	2.69 ± 1.05	8.76 ± 6.81
Heme + TAK-242	7.8 ± 0.20	26.53 ± 0.91

HUVECs were treated with heme (2.5 μM) in the presence or absence of the NF-κB signaling inhibitor, Bay-11082 (5 μM) or the TLR4 signaling inhibitor, TAK-242 (1 μM) for 9 h. Expression of VCAM1 and ICAM1 was analyzed by real time RT-PCR and normalized to the expression of HPRT. Values are represented as mean ± SD fold induction in relation to control unstimulated cells. One-way ANOVA with Tukey's post-hoc analysis was performed for statistical analyses; VCAM-1 (Heme vs others **p < 0.01) and ICAM-1 (Heme vs others **p < 0.01).

in lysosomes.

2.6. A1AT blocks heme-mediated lysosomal alkalization

To further investigate the role of A1AT in ECs, we performed additional experiments with acridine orange (AO), a lysosomotropic dye. Treatment with heme alone caused a marked decrease in lysosomal AO staining, but this was not observed in the presence of A1AT (Fig. 6A). The decrease in AO fluorescence intensity by heme and its recovery by A1AT was also determined and quantified by flow cytometry (Fig. 6B). To corroborate that heme induces lysosomal alkalization ECs were stained with LysoSensor Green, a pH-dependent indicator probe. Stimulation of ECs with heme caused a marked decrease in the intensity of LysoSensor Green that was counter-acted by A1AT (Fig. 6C). In an attempt to re-acidify lysosomes, ECs were pretreated with forskolin, an inducer of cAMP [37]. Heme-mediated decrease in fluorescence intensity of LysoSensor Green was partially reversed by treatment with forskolin (Fig. 6D). Moreover, MTT assays revealed that forskolin significantly improves the viability of heme-treated ECs (Fig. 6E). Collectively, these findings indicate that heme causes lysosomal alkalization in ECs that is prevented by A1AT.

2.7. A1AT rescues heme-dependent dysfunction of autophagy in ECs

Lysosomes play a key role in autophagy, a process that is necessary for maintaining cellular homeostasis [38]. A significant increase in levels of the autophagy marker protein microtubule light chain (LC)3BII was observed in heme-treated ECs (Fig. 7A). In parallel, up-regulation of p62, also known as SQSTM1, was observed indicating an inhibition of

autophagosome degradation (Fig. 7A). Heme-induced up-regulation of LC3BII and p62 was suppressed by A1AT (Fig. 7A). The addition of the lysosomal inhibitor chloroquine to non-treated or A1AT-treated ECs, and that of rapamycin, a positive control for autophagy, led to an increase in LC3BII indicating a normal autophagic flux (Fig. 7B). By contrast, chloroquine added to heme-treated cells failed to increase LC3BII levels indicating diminished autophagic flux (Fig. 7B). Moreover, the staining with cytoID revealed an accumulation of autophagosomes in heme-treated ECs, but not in heme plus A1AT-treated cells (Fig. 7C). Finally, we asked if distinct alterations of autophagy-associated pathways may affect cytoprotection against heme toxicity by A1AT. To this end, two lysosomal acidification blockers, concanamycin-A and bafilomycin-A1, as well as two autophagosome formation blockers, wortmannin (a phosphatidylinositol-3 kinase (PI3K) inhibitor) and MRT68921 (an Unc-51 like autophagy activating kinase (ULK) inhibitor) were applied. Inhibitors of lysosomal acidification, but not those of autophagosome formation, markedly enhanced cell death (Fig. 7D and E). When combined with lysosomal inhibitors, heme exerted an additive cytotoxic effect, which was not observed with two other inhibitors of autophagy (Fig. 7D and E). Notably, cytoprotective effects of A1AT against heme toxicity were preserved in the presence of autophagy inhibitors but partially lost in the presence of the lysosomal inhibitors (Fig. 7D and E) suggesting that reversal of lysosomal alkalization rather than direct correction of autophagy is responsible for inhibition of heme-induced cell death.

3. Discussion

Vascular ECs control blood vessel homeostasis and play a critical role in the pathogenesis of inflammatory disorders [1]. In various clinical conditions such as sickle cell disease, sepsis or IRI, high levels of extracellular free heme can arise from hemolysis or tissue damage and cause endothelial injury, dysfunction or death via pro-oxidant, pro-inflammatory and cytotoxic effects [4,5,9]. In the current study, we show that human A1AT, an acute phase protein with high binding affinity for heme ($K_D \sim 10^{-7}$ M) [26], protects against free heme toxicity in ECs via a mechanism different from that of albumin and hemopexin, two major serum HBPs. In contrast to these latter proteins, A1AT has protective effects without blocking the cellular up-take of heme. Furthermore, we provide experimental evidence that A1AT-dependent protection against heme in ECs is mediated via pathways that block EC activation, death and dysfunction of autophagy.

Exposure to low concentrations of heme can cause activation of ECs with increased expression of adhesion molecules and cytokine production [28] whereas higher concentrations of heme can cause EC death [30,39]. We show that A1AT counteracts heme-induced EC activation and death (Figs. 1 and 2). According to previous reports, heme scavenger proteins such as albumin and hemopexin protect the endothelium via blocking the cellular uptake of heme [31]. By contrast, A1AT does not inhibit the up-take of heme by ECs and heme-mediated up-regulation of HO-1, an inducible heme-degrading enzyme (Fig. 3). Because HO-1 overexpression is known to be protective in the vascular endothelium [40], we assumed that the up-regulation of HO-1 by heme and A1AT may be critical for A1AT-dependent protection against heme toxicity. However, blockage of HO enzyme activity or silencing of HO-1 gene expression, did not affect A1AT's ability to inhibit the toxicity of heme (Fig. 3). Therefore, the protective effects of A1AT appear to be independent of heme degradation by HO-1.

Laser confocal microscopy assays revealed that extracellular free heme strongly enhanced A1AT uptake by ECs (Fig. 5A). It is also important to note that heme increased endothelial up-take of purified A1AT (Fig. 5A) and also that of A1AT from whole human plasma (Fig. 5B). ECs lack the ability to synthesize their own pool of intracellular A1AT and are entirely dependent on circulating levels of A1AT. Previous studies have shown that A1AT is internalized by ECs in a time-, dose- and conformation-dependent manner. Moreover, internalization

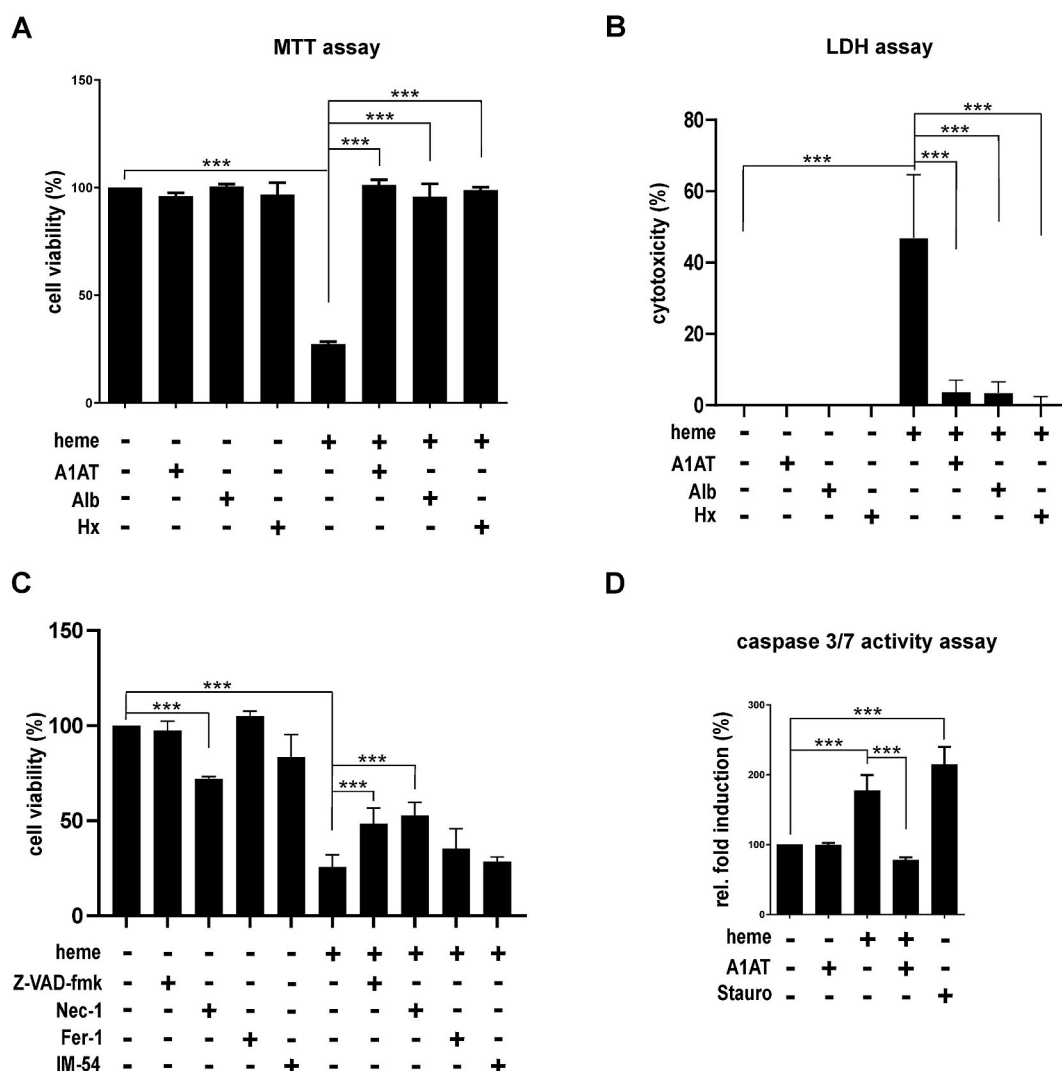


Fig. 2. A1AT blocks heme-induced EC death. The viability of HUVECs treated with heme (2.5 μ M) in the presence of A1AT (0.5 mg/ml), albumin (Alb) (0.5 mg/ml) or hemopexin (Hx) (0.5 mg/ml) for 18 h was assessed by (A) MTT assay and LDH assay (B). (C) The viability of HUVECs stimulated with heme (2.5 μ M) in the presence of z-VAD-fmk (50 μ M), necrostatin-1 (nec-1) (50 μ M), ferrostatin-1 (fer-1) (10 μ M) or IM-54 (10 μ M) was assessed by MTT assay (D) HUVECs treated for 12 h were subjected to caspase 3/7 activity measurements as detailed in Materials and Methods. Staurosporine (0.75 μ M), an inducer of apoptosis was used as a positive control. Results shown are means \pm SEM of at least three independent experiments. One-way ANOVA with Tukey's post-hoc analysis was performed for statistical analysis, *** p < 0.001. Alb, albumin; Hx, hemopexin.

of A1AT has been demonstrated to be mediated via both clathrin- and caveolae-mediated endocytosis [41,42]. The increased up-take of A1AT by ECs in the presence of extracellular free heme (Fig. 5) supports a protective nature of this event and the mechanisms of how heme mediates the intracellular up-take of A1AT in ECs warrant further investigation.

More detailed microscopy studies indicated that A1AT is localized in lysosomes (Fig. 5). In addition, heme caused lysosomal alkalization via a yet unknown mechanism, which was markedly inhibited in the presence of A1AT (Figs. 5 and 6). Previously, apolipoprotein D has been demonstrated to reduce lysosomal permeabilization and to stabilize the pH of these organelles resulting in a significant improvement of cell viability [43]. Therefore, it is tempting to speculate that the effect of A1AT might be similar to that of apolipoprotein D. Further studies are required to find out if A1AT's property to maintain lysosomal alkalization is associated with binding of free heme or direct lysosomal interactions.

Lysosomal alkalization can lead to alterations of the autophagy pathway [44,45] that is important for cell homeostasis [46]. Therefore, diminution or blockage of autophagy can result in intracellular

accumulation of misfolded proteins and dysfunctional organelles [47]. Indeed, heme-induced lysosomal alkalization appeared to coincide with impaired autophagy in ECs (Fig. 7) as observed by the decrease in autophagy flux (Fig. 7) [48], which was rescued in the presence of A1AT. It should be noted that earlier findings on the effects of free heme and autophagy are contradictory. Heme has been shown to block autophagy flux in cardiomyocytes and to induce cytotoxicity [49]. On the other hand, heme has been shown to induce autophagy, which was then considered a protective mechanism in bovine aortic ECs [50].

Free heme concentrations in human plasma may range between 2 and 5 μ M, as determined with an antibody-based assay [51]. Thus, heme concentrations used in our study are relatively low (2.5 μ M) as compared to those in previous reports (10 μ M and higher). These latter differences may, at least in part, explain discrepancies between studies on the heme effects in autophagy. Similar to heme, A1AT has also been reported to play contrasting roles in the regulation of autophagy. Endogenous A1AT has previously been shown to act as a negative regulator of autophagy in cultured breast cancer cells [52]. By contrast, in human macrophages A1AT has been reported to enhance autophagy upon mycobacterial infection [53]. The mechanistic details on how

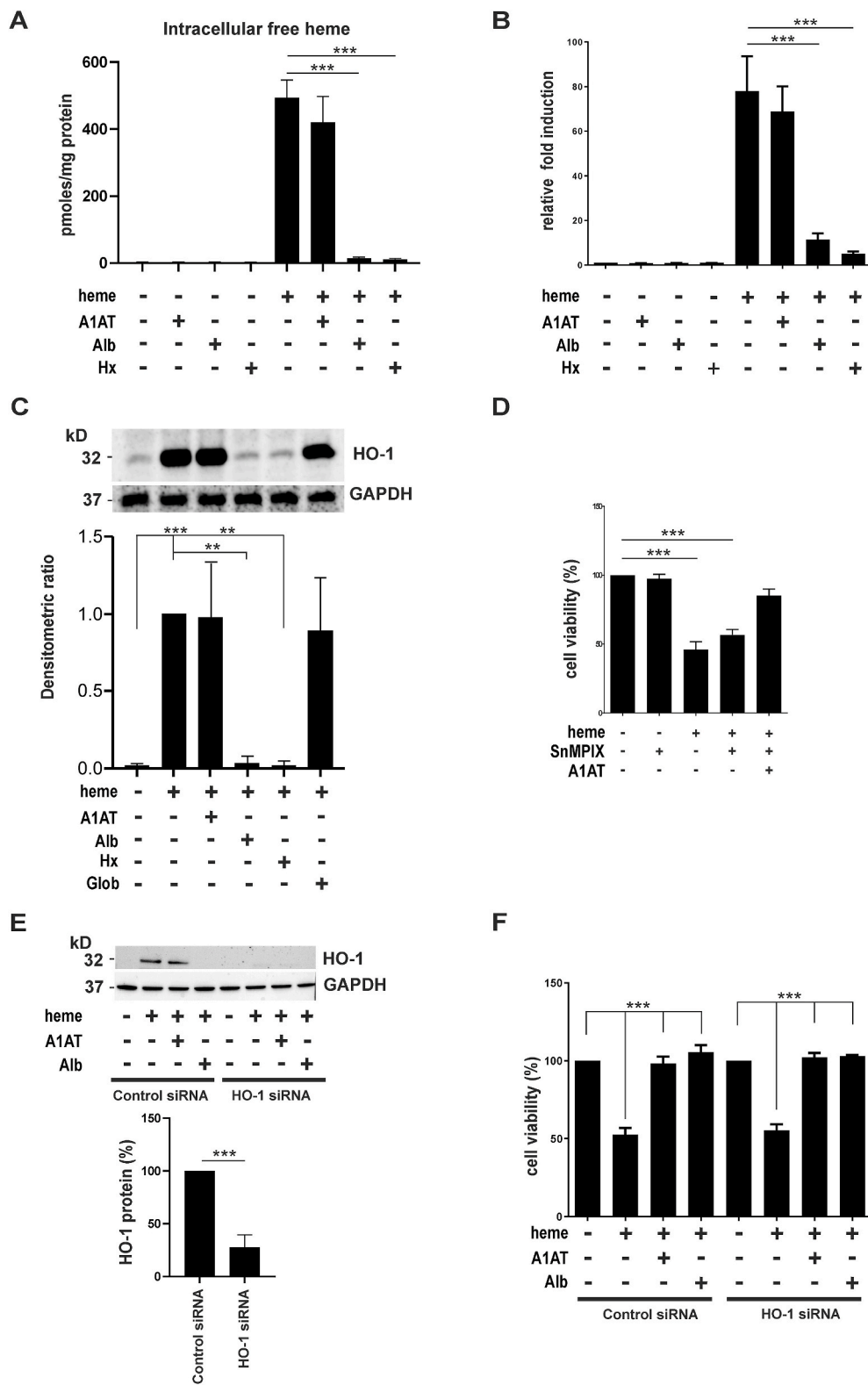


Fig. 3. A1AT mediated protection against heme toxicity is independent of HO-1. (A–C) HUVECs were treated as indicated for 4 h. (A) Intracellular free heme was measured using an apo-HRP assay as detailed in Materials and Methods. (B) RNA isolated was analyzed by real-time RT-PCR for the expression of HO-1 and normalized to the expression of HPRT. (C) A representative Western blot of total cell lysates probed with antibodies against HO-1 and GAPDH (Top) and a bar graph that represents the mean of densitometric quantification normalized to GAPDH from three independent experiments is shown as fold change in relation to heme-induced HO-1 expression (bottom). (D) HUVECs were pretreated with SnMPIX (10 μ M) for 1 h before adding heme (2.5 μ M) and A1AT (0.5 mg/ml), as indicated, for another 18 h. Cell viability was assessed by MTT assay. (E) A representative Western blot of total cell lysates probed with the antibodies against HO-1 and GAPDH isolated from cells transfected with the indicated siRNA for 48 h followed by 4 h of treatment with heme (2.5 μ M) (Top) and a comparison of HO-1 densitometric quantification in heme-treated control and HO-1 siRNA transfected lanes is shown as a bar graph (Bottom). The values are normalized to GAPDH and represents the mean of at least three independent experiments (F) HUVECs transfected with the indicated siRNAs were treated with heme (2.5 μ M) and A1AT (0.5 mg/ml) and subjected to MTT assays as described in Materials and Methods. Results shown are mean of at least three independent experiments. Student's t-test or one-way ANOVA with Tukey's post-hoc analysis was performed for statistical analyses, ** $p < 0.01$, *** $p < 0.001$. Alb, albumin; Hx, hemopexin; Glob, γ -globulin.

A1AT corrects heme-induced autophagy needs to be explored further. The current results allow to conclude that A1AT interacts with various heme-dependent pro-oxidant and pro-inflammatory pathways that cause EC activation, death and impairment of autophagy all of which may not necessarily be linked with each other. It is conceivable that A1AT can prevent EC activation via inhibiting NF- κ B signaling whereas EC death is blocked by reduction of mROS production, caspase

activation and lysosomal alkalization. Although most recognized for its inhibitory role on neutrophil elastase and proteinase 3, A1AT also exhibits a number of other anti-inflammatory and immunomodulatory cell-type specific functions [54]. For example, A1AT has been shown to inhibit caspase activity and to prevent EC death [55] which is in line with findings of the current report. Increased intracellular levels of A1AT in the presence of heme (Fig. 5) could be a protective mechanism

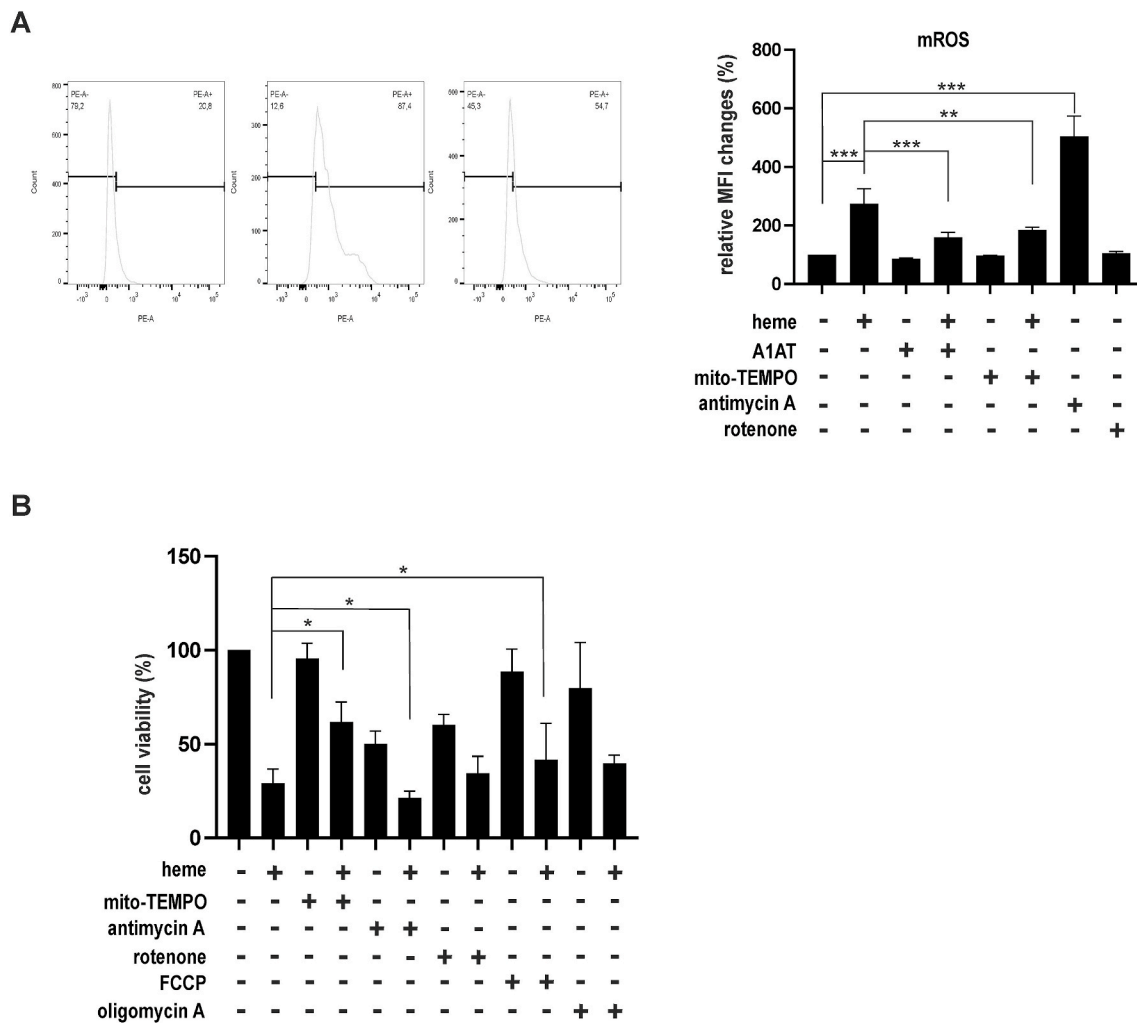


Fig. 4. A1AT blocks heme-induced mitochondrial ROS production. (A–B) HUVECs were treated with heme (2.5 μ M) in the presence of A1AT (0.5 mg/ml), mito-TEMPO (75 μ M), antimycin-A (4 μ M), rotenone (1 μ M), FCCP (1 μ M) and oligomycin A (2 μ M) for 3 h (A) or 18 h (B), as indicated. (A) A representative histogram of mitochondrial ROS levels assessed by flow cytometry using MitoSox (left) and the percentage changes in relative mean fluorescence intensity (MFI) shown as a bar graph. (B) Cell viability was assessed by MTT assays. Values represent mean \pm SEM of at least three independent experiments. One-way ANOVA with Tukey's post-hoc analysis was performed for statistical analysis, * p < 0.05, ** p < 0.01, *** p < 0.001.

that might be of particular relevance in pathophysiological situations, in which the heme-binding capacities of albumin and hemopexin are exhausted or high levels of free heme occur as a consequence of tissue damage by IRI or other pathophysiological conditions [9]. Recent studies have shown that A1AT has protective effects against renal IRI by inhibiting pathways of inflammation and apoptosis [56]. It is conceivable that these effects of A1AT may be related to its free heme-neutralizing properties.

Hence, we provide novel aspects of how the acute-phase protein A1AT, a recently identified HBP, can exert protection of ECs against the toxicity of extracellular free heme. Our findings expand knowledge on some as yet unknown functions of A1AT in pathophysiological settings, in which large amounts of free heme are released. The ability of A1AT to counter-act clinically relevant toxicity of free heme in the endothelium may help to develop novel therapeutic applications of A1AT for the treatment of disorders associated with hemolysis or tissue damage.

4. Materials and methods

4.1. Reagents

A1AT was purchased from CSL Behring (Kankakee, IL, USA), human-serum albumin (HSA) from Octapharma (Lachen, Switzerland) and

human hemopexin from Athens research and technology (Athens, GA, USA). Hemin and SnMPIX were obtained from Frontiers Scientific (Logan, UT, USA). IM-54 and Z-VAD-fmk were purchased from Santa Cruz Biotechnology (Dallas, TX, USA). All other materials and reagents were obtained from Sigma-Aldrich (St. Louis, MO, USA) or Tocris Bioscience (Bristol, UK), unless otherwise indicated.

4.2. Cell culture

Human umbilical vein endothelial cells (HUVECs) (3 independent donors), human aortic endothelial cells (HAoECs), human pulmonary microvascular endothelial cells (HPMVECs) and human dermal microvascular endothelial cells (HDMVECs) (2 independent donors, respectively) were purchased from PromoCell (Heidelberg, Germany). HUVEC and HAoEC were cultivated in endothelial cell growth medium (PromoCell) with supplements including 2%/5% heat-inactivated fetal calf serum, respectively and used in passages 4 to 7. HPMVEC and HDMVEC were cultivated in endothelial cell growth medium MV (PromoCell) with supplements and 5% heat-inactivated fetal calf serum and used in passages 4 to 7. Cells were maintained at 37 $^{\circ}$ C, 5% CO₂ and 100% humidity until confluence. For the experiments, ECs were plated in 12 well plates at a seeding density of 1.5×10^5 cells/well or in 24 well plates at a seeding density of 8×10^4 cells/well. Except for immunofluorescence

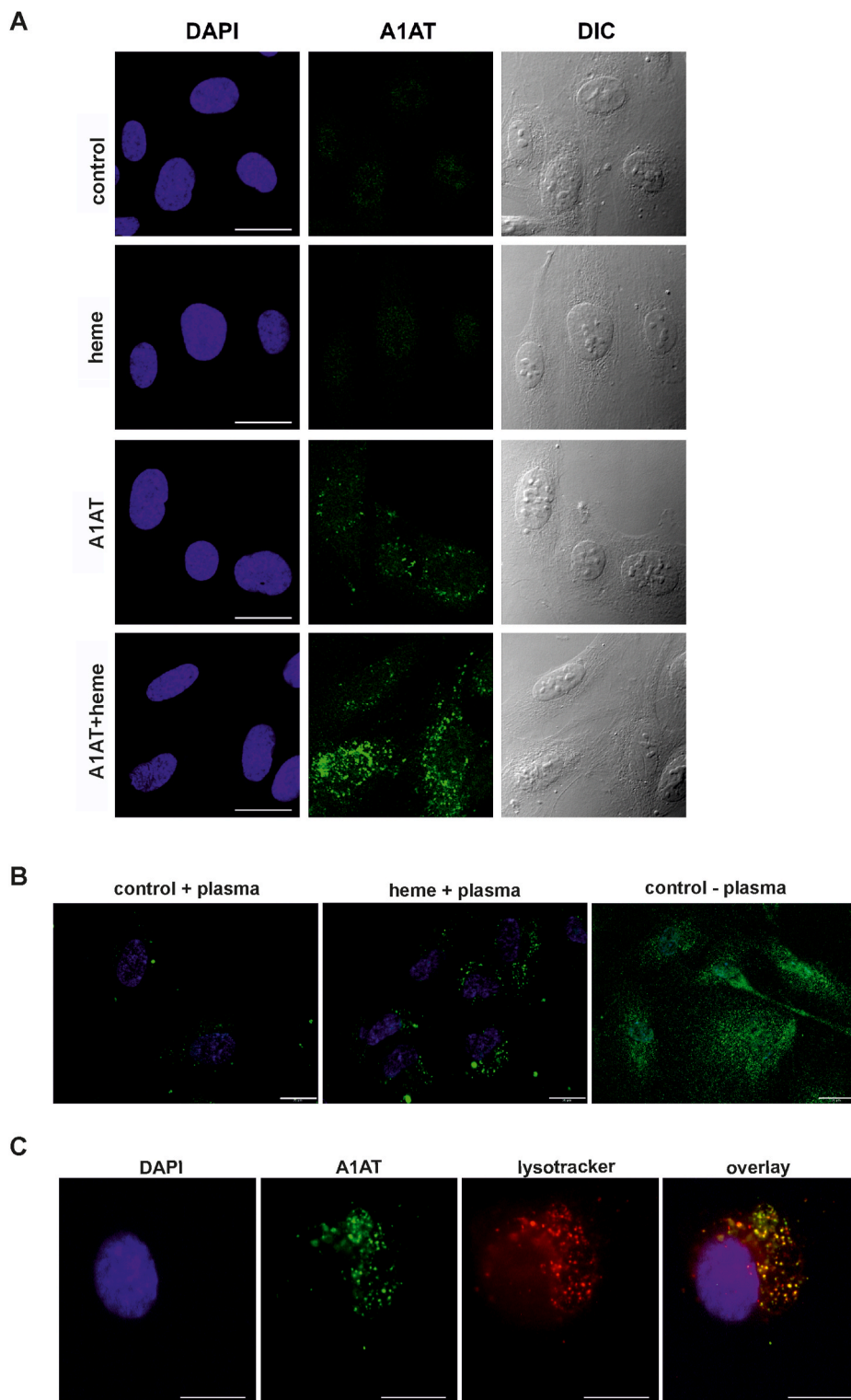


Fig. 5. Heme-mediated up-take of extracellular A1AT in ECs. (A–B) HUVECs were treated for 4 h with heme (2.5 μ M) and A1AT (0.5 mg/ml) as indicated. (A) A representative confocal microscopy image of cells stained with an antibody against A1AT is shown. Nuclei were stained with 4',6-diamidin-2-phenylindol (DAPI, 1 μ g/ml). (B) A representative fluorescence microscopy image of HUVECs treated with heme (2.5 μ M) in medium supplemented with native human plasma (10%) for 4 h and stained with DAPI and an antibody against A1AT (Bar = 20 μ m) is shown. (C) A representative fluorescence microscopy image of cells co-stained with LysoTracker Red, DAPI and an antibody against A1AT (Bar = 20 μ m) is shown. Colocalization of A1AT and lysosomes were calculated using Image J (Pearson's r value = 0.79 ± 0.075). All images are representatives of at least three independent experiments. (For interpretation of the references to colour in this figure legend, the reader is referred to the Web version of this article.)

studies, cells were used for the experiment when it reached a desired confluency of 75–80%. The final molar concentration of serum proteins A1AT, hemopexin and albumin used for experiments were 9.62 μ M, 8.47 μ M and 7.52 μ M respectively, corresponding to a concentration of 0.5 mg/ml in either 1 ml of medium/well for 12 well plates or 0.5 ml/well for 24 well plates.

4.3. 3-(4, 5-dimethylthiazol-2-yl)-2,5-diphenyltetrazolium bromide (MTT) assay

MTT assay was performed as described previously [57]. Briefly, the medium was replaced with fresh serum free medium supplemented with MTT (0.5 mg/ml, Sigma-Aldrich, St. Louis, MO, USA) and incubated at 37 $^{\circ}$ C for 2 h. The resulting formazan crystals were dissolved in DMSO and absorbance read at 570 nm using a spectrophotometer (Biotek). The cell viability was calculated by the following formula: A570 of treated

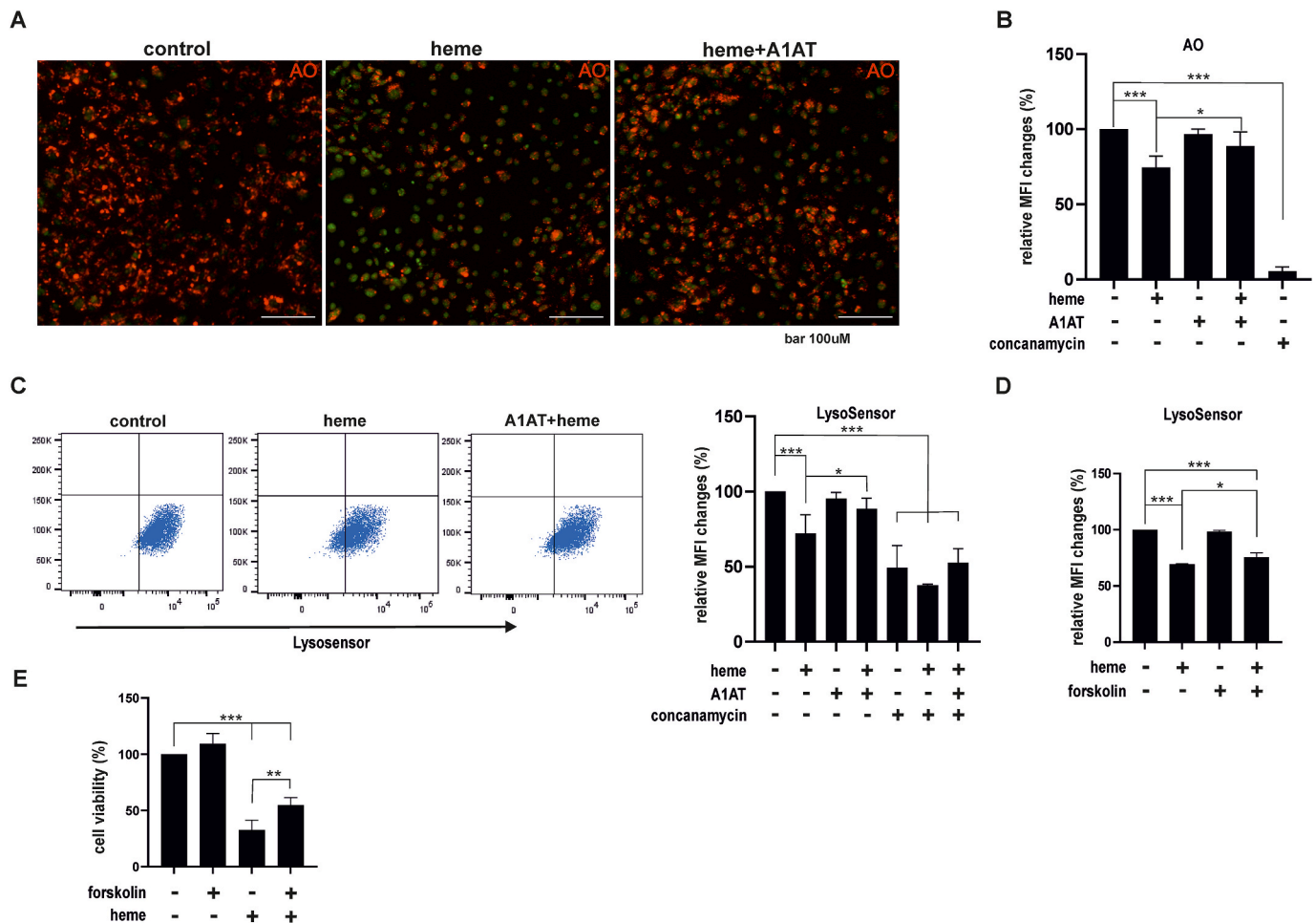


Fig. 6. Heme-induced lysosomal alkalization is reduced by A1AT. (A–E) HUVECs were treated with heme (2.5 μ M) in the presence A1AT (0.5 mg/ml) or concanamycin (0.1 μ M) as indicated for 4 h. (A) A representative fluorescence image of acridine orange (AO) staining as mentioned in Materials and Methods (Bar = 100 μ m) is shown. (B) Relative changes in AO staining of ECs as determined by flow cytometry are shown in % of MFI. (C) A representative dot plot of ECs stained with LysoSensor Green assessed by flow cytometry (left) and relative changes (% of MFI) (right) are shown. (D) HUVECs were pretreated with forskolin (10 μ M) for 1 h before addition of heme for another 4 h (2.5 μ M), as indicated. Cells were stained with lysosensor and analyzed by flow cytometry. (E) HUVECs were pre-treated with forskolin (10 μ M) for 1 h before stimulation with heme (2.5 μ M) for an additional 18 h. Cell viability was assessed by MTT assays. Values represent mean \pm SEM of at least three independent experiments. One-way ANOVA with Tukey's post-hoc analysis was performed for statistical analyses, * p < 0.05, ** p < 0.01, *** p < 0.001. (For interpretation of the references to colour in this figure legend, the reader is referred to the Web version of this article.)

cells/A570 of non-treated cells \times 100.

4.4. Lactate dehydrogenase (LDH) assay

The amount of LDH released in the cell culture supernatant was determined using Cytotoxicity Detection Kit Plus (Roche, Basel, Switzerland) according to the manufacturer's protocol.

4.5. Western blot

Western blotting was performed with primary antibodies against HO-1 (1:1,000, Enzo Life Sciences, Farmingdale, NY, USA), phospho65 (1:1,000, Cell Signaling Technology, Danvers, MA, USA), LC3B (1:1,000, Sigma-Aldrich, St. Louis, MO, USA), β -actin (1:5,000, Sigma-Aldrich) and secondary horse radish-conjugated goat anti-rabbit or rabbit anti-mouse (1:4,000, Agilent Dako, Santa Clara, CA, USA), as previously described. Signals were visualized by Clarity Western ECL Substrate (Bio-Rad, Hercules, CA, USA) and quantified with a ChemiDoc MP Imaging System (Bio-Rad). Images were processed using Corel Draw Graphic Suite \times 5 Software (Corel Corporation, Ottawa, Canada).

4.6. Analysis of mRNA expression

RNA isolation was performed using an RNeasy mini kit (Qiagen GmbH, Hilden, Germany). Synthesis of cDNA was performed by employing High Capacity cDNA Reverse Transcription Kit (Applied Biosystems, Carlsbad, CA, USA). Inventoried primers for quantification of mRNA levels of VCAM-1, ICAM-1, IL-8, HO-1 and hypoxanthine phosphoribosyltransferase 1 (HPRT) were purchased from Applied Biosystems. Amplification was performed with TaqMan Gene Expression Master Mix on a StepOnePlus™ Real-Time PCR System (Applied Biosystems, Carlsbad, CA, USA). Thermal cycling was performed at 95 $^{\circ}$ C for 10 min followed by 40 cycles at 95 $^{\circ}$ C for 15 s and 60 $^{\circ}$ C for 1 min. HPRT was used as a control for normalization of cDNA values. The $\Delta\Delta$ CT method was used to semi-quantify mRNA levels.

4.7. Immunofluorescence

Cells plated on coverslips in 24-well plates were subjected to an indirect immunofluorescence staining protocol as previously described [58]. Briefly, at the end of the experiment cells were washed with PBS and fixed using 4% paraformaldehyde and 2% saccharose for 20 min, following permeabilization using 1% glycine containing 0.02% Triton

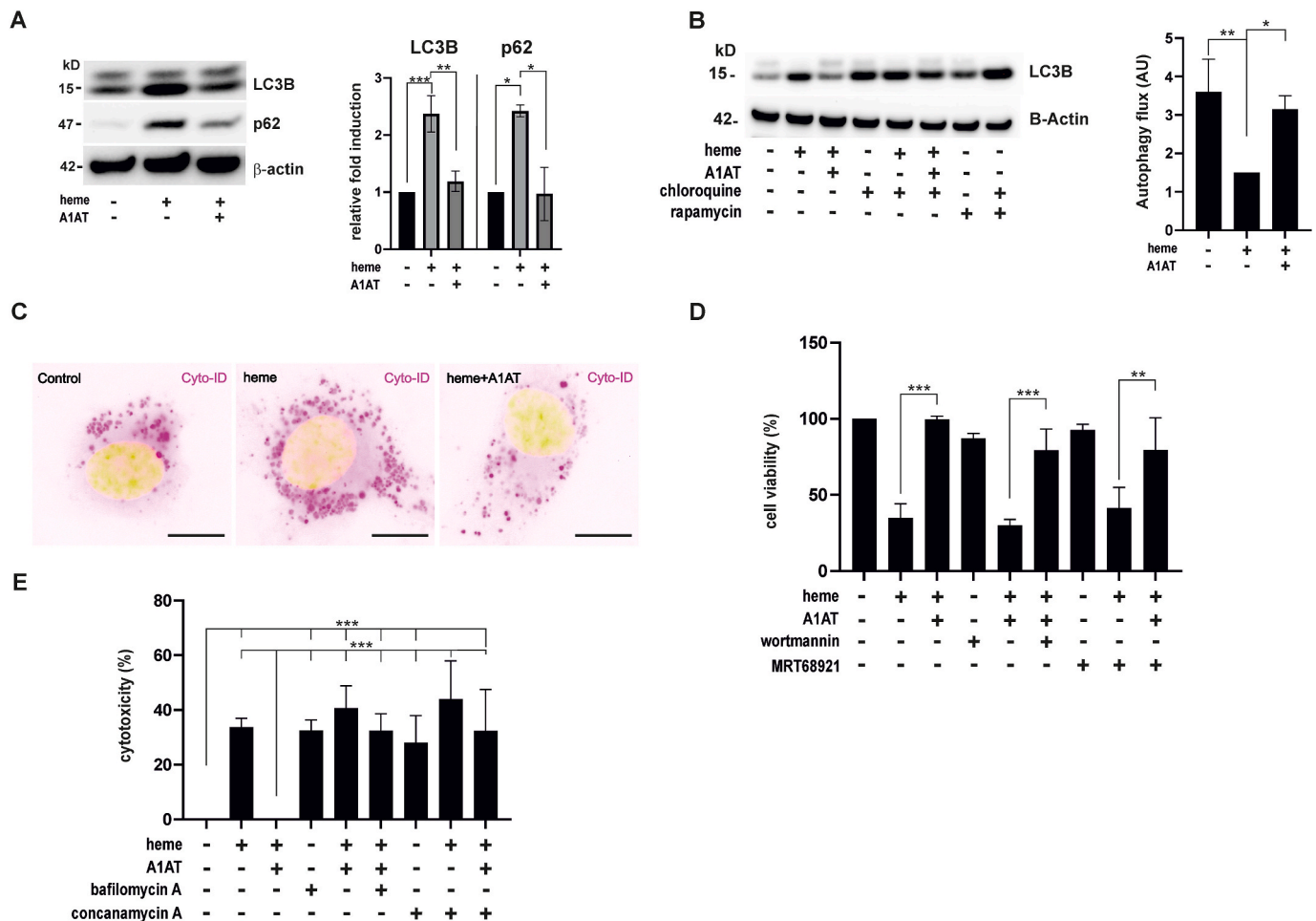


Fig. 7. A1AT corrects heme-induced autophagy dysfunction. (A–C) HUVECs were treated with heme (2.5 μ M) in the presence of A1AT (0.5 mg/ml) and chloroquine (0.1 mM), rapamycin (500 nM) for 8 h, as indicated. (A–B) Representative Western blots of total cell lysates using antibodies against LC3B/II, p62 and β -actin. (C) A representative image of cyto-ID staining (bar = 20 μ m) is shown. (D–E) HUVECs pretreated with the lysosomal inhibitors bafilomycin A (25 nM), concanamycin A (0.1 μ M) or the autophagy inhibitors wortmannin (1 μ M), MRT68921 (1 μ M) for 1 h before heme treatment for another 18 h. Cell viability was determined with MTT and LDH assays, respectively. Values represent mean \pm SEM of at least three independent experiment). One-way ANOVA with Tukey's post-hoc analysis was performed for statistical analyses, * p < 0.05, ** p < 0.01, *** p < 0.001.

X-100 for an additional 10 min. Next, cells were washed using PBS containing 0.05% Tween. Non-specific binding sites were blocked with 1% bovine serum albumin prepared in washing buffer for 30 min at room temperature. The primary antibody against A1AT was incubated overnight at 4 $^{\circ}$ C followed by incubation with an Alexa Fluor 488-conjugated secondary antibody at 1:500 dilution (Invitrogen). Nuclei were visualized with 1 μ M Hoechst 33,342 for 5 min at RT embedded in Mowiol 4–88. All samples were inspected with an Olympus IX81 microscope equipped with a DR4 camera. Digital pictures were processed with image J software. For confocal microscopy images were acquired using confocal laser microscope Olympus FluorView 1000 equipped with a 60 \times oil immersion objective in sequential mode.

4.8. Apo-horseradish peroxidase (HRP) assay to determine intracellular heme levels

Intracellular levels of free heme were determined with a method based on the reconstitution of apo-HRP as described previously [59]. The assay works on the principle that amount of free transferable heme is directly proportional to the amount of active form of HRP (holo-HRP) formed when an inactive form (non-heme containing or apo-HRP) is supplied. A heme standard was used to determine the concentration of heme in the cell lysates based on the holo-HRP activity. 2–40 μ L of protein cell lysates from each sample were added to the required amount

of HBSS to get an initial volume of 50 μ L. From a 10 nM heme stock solution, a heme standard curve with concentrations of 0.25, 0.5, 1, 1.5, 2.0 and 2.5 nM for a reaction volume of 100 μ L was calculated and prepared initially in 50 μ L. Next, 50 μ L of 750 nM apo-HRP (APO-HRP4C; BBI Solution, Gwent, UK), was added to all the samples and standards. The reconstitution reaction was carried out in a 96-well plate for 10 min at 4 $^{\circ}$ C. Following incubation, 5 μ L of each reaction was transferred to a new 96-well plate. The holo-HRP activity of the samples and standards were recorded by adding 200 μ L of TMB substrate (KEM-EN-TEC Diagnostics, Copenhagen, Denmark) and measuring the absorbance at 652 nm kinetically on a BioTek Synergy 2 (Agilent Bio-Tek, Winooski, VT, USA) plate reader until the absorbance of the highest standard was between 1.5 and 1.8. Unknown labile heme concentrations in the cell lysate were calculated from the linear regression analysis of the heme standard curve and normalized to protein concentrations in cell lysates. The final free heme values are expressed as pmoles/mg protein.

4.9. Caspase 3/7 activity assay

Caspase 3/7 activity assay kit (Promega, Madison, WI, USA) was used according to the manufacturer's protocol.

4.10. Mitochondrial ROS (mROS) production

HUVECs (0.75×10^5 cells/well) were plated in 24-well plates and allowed to rest overnight. The following day medium was replaced with serum free medium and cells were stimulated for 3 h with different reagents as detailed in the respective Figure Legends. The medium was replaced with a fresh serum free medium containing 5 μ M of Mitosox (Thermo Fisher Scientific, Inc. Waltham, MA, USA) and incubated for 10 min followed by FACS analysis.

4.11. Autophagy flux measurement

To calculate the autophagy flux the densitometry values of LC3BII was determined and respective fold induction in relation to the band in control unstimulated cells were calculated. The autophagy flux was determined by subtracting the fold induction values of chloroquine treatment and the respective treatment without chloroquine.

4.12. CytoID staining

HUVECs (1×10^5 cells/well) plated on coverslips in a 24 well plate were treated with heme in the presence or absence of A1AT for 6 h followed by CytoID staining (CYTO-ID® Autophagy detection kit, Enzo Life Sciences, Farmingdale, NY, USA) according to the manufacturer's protocol. Pictures were taken using an Olympus IX81 microscope equipped with a DR4 camera. Digital pictures were processed with image J software.

4.13. Lysosomal parameters (acridine orange (AO), LysoTracker red and LysoSensor green)

HUVECs (0.75×10^5 cells/well) were cultured in 24-well plates and allowed to rest overnight. At the end of the experiment, the medium was replaced with fresh serum free medium containing AO (2 μ M), LysoTracker Red (50 nM, Life Technologies, Carlsbad, CA, USA) or LysoSensor Green (1 μ M, Life Technologies) and incubated for further 20 min. Cells were analyzed by flow cytometry or by fluorescence microscopy as described previously [60]. For co-localization experiments, LysoTracker Red staining was performed before fixing the cells.

4.14. Knockdown experiments

HUVECs were transfected in 12-well plates with 75 nM of HO-1 small interfering RNA (siRNA) (ID:s194530) from Thermo Fischer Scientific, and control siRNA (Pre-designed validated AllStars Negative Control siRNA, Qiagen, Venlo, Netherlands) using ScreenFect A-plus transfection reagent (Incella, Eggenstein-Leopoldshafen, Germany) according to the manufacturer's instructions. The knockdown was verified by Western blot analyses after 48 h of transfection.

4.15. Flow cytometry analysis

Flow cytometry analysis was performed on a FACS Canto II flow cytometer (Becton, Dickinson and Company, Franklin Lakes, NJ, USA) and quantification was performed using FACS Diva software.

4.16. Statistical analyses

All statistical data analysis was performed using One-way ANOVA with Post Tukey's test or Student's *t*-test as indicated in the figure legends using GraphPad Prism Version 8 (GraphPad Prism Software Inc.).

Funding

This work was supported by funding by the Deutsche Forschungsgemeinschaft (IM 20/4-1) and the European Union and the State

of Niedersachsen project EFRE ZW6-85007634 (to SI).

Author contributions

VV, SJ and SI designed the outline and experiments of the study. KM, VV, CN, AA, ST, EK, HS, HF and MS conducted experiments. KM, VV, SJ, and SI wrote the manuscript.

Declaration of competing interest

The author's state no conflict of interest.

Acknowledgements

We would like to thank Anette Sarti-Jacobi for technical assistance.

Appendix A. Supplementary data

Supplementary data to this article can be found online at <https://doi.org/10.1016/j.redox.2021.102060>.

References

- [1] J.S. Pober, W. Min, J.R. Bradley, Mechanisms of endothelial dysfunction, injury, and death, *Annu. Rev. Pathol.* 4 (2009) 71–95.
- [2] J.A. Vita, Endothelial function, *Circulation* 124 (2011) e906–912.
- [3] W.C. Aird, Phenotypic heterogeneity of the endothelium: II. Representative vascular beds, *Circ. Res.* 100 (2007) 174–190.
- [4] S. Kumar, U. Bandyopadhyay, Free heme toxicity and its detoxification systems in human, *Toxicol. Lett.* 157 (2005) 175–188.
- [5] M. Frimat, I. Boudhabhay, L.T. Roumenina, Hemolysis derived products toxicity and endothelium: model of the second hit, *Toxins* 11 (2019).
- [6] J. Balla, G.M. Vercellotti, V. Jeney, A. Yachie, Z. Varga, H.S. Jacob, J.W. Eaton, et al., Heme, heme oxygenase, and ferritin: how the vascular endothelium survives (and dies) in an iron-rich environment, *Antioxidants Redox Signal.* 9 (2007) 2119–2137.
- [7] D.J. Schaer, P.W. Buehler, A.I. Alayash, J.D. Belcher, G.M. Vercellotti, Hemolysis and free hemoglobin revisited: exploring hemoglobin and heme scavengers as a novel class of therapeutic proteins, *Blood* 121 (2012) 1276–1284.
- [8] M.P. Soares, M.T. Bozza, Red alert: labile heme is an alarmin, *Curr. Opin. Immunol.* 38 (2016) 94–100.
- [9] S. Immenschuh, V. Vijayan, S. Janciauskiene, F. Gueler, Heme as a target for therapeutic interventions, *Front. Pharmacol.* 8 (2017) 146.
- [10] V. Jeney, J. Balla, A. Yachie, Z. Varga, G.M. Vercellotti, J.W. Eaton, G. Balla, Pro-oxidant and cytotoxic effects of circulating heme, *Blood* 100 (2002) 879–887.
- [11] J.D. Belcher, C. Chen, J. Nguyen, L. Milbauer, F. Abdulla, A.I. Alayash, A. Smith, et al., Heme triggers TLR4 signaling leading to endothelial cell activation and vaso-occlusion in murine sickle cell disease, *Blood* 123 (2014) 377–390.
- [12] E. Merle, R. Paule, J. Leon, M. Daugan, T. Robe-Rybikine, V. Poillierat, C. Torset, et al., P-selectin drives complement attack on endothelium during intravascular hemolysis in TLR-4/heme-dependent manner, *Proc. Natl. Acad. Sci. U.S.A.* 116 (2019) 6280–6285.
- [13] S. Janciauskiene, V. Vijayan, S. Immenschuh, TLR4 signaling by heme and the role of heme-binding blood proteins, *Front. Immunol.* 11 (2020) 1964.
- [14] R.K. Donegan, C.M. Moore, D.A. Hanna, A.R. Reddi, Handling heme: the mechanisms underlying the movement of heme within and between cells, *Free Radic. Biol. Med.* 133 (2019) 88–100.
- [15] S.H. Vincent, R.W. Grady, N. Shaklai, J.M. Snider, Muller-Eberhard, The influence of heme-binding proteins in heme-catalyzed oxidations, *Arch. Biochem. Biophys.* 265 (1988) 539–550.
- [16] I. Hamza, H.A. Dailey, One ring to rule them all: trafficking of heme and heme synthesis intermediates in the metazoans, *Biochim. Biophys. Acta* 1823 (2012) 1617–1632.
- [17] H.H. Brewitz, G. Hagelueken, D. Imhof, Structural and functional diversity of transient heme binding to bacterial proteins, *Biochim. Biophys. Acta Gen. Subj.* 1861 (2017) 683–697.
- [18] M. Paoli, B.F. Anderson, H.M. Baker, W.T. Morgan, A. Smith, E.N. Baker, Crystal structure of hemopexin reveals a novel high-affinity heme site formed between two beta-propeller domains, *Nat. Struct. Biol.* 6 (1999) 926–931.
- [19] E. Tolosano, F. Altruda, Hemopexin: structure, function, and regulation, *DNA Cell Biol.* 21 (2002) 297–306.
- [20] U. Muller-Eberhard, H. Cleve, Immunoelectrophoretic studies of the beta1-haem-binding globulin (haemopexin) in hereditary haemolytic disorders, *Nature* 197 (1963) 602–603.
- [21] U. Muller-Eberhard, J. Javid, H.H. Liem, A. Hanstein, M. Hanna, Plasma concentrations of hemopexin, haptoglobin and heme in patients with various hemolytic diseases, *Blood* 32 (1968) 811–815.

- [22] D. Chiabrando, F. Vinchi, V. Fiorito, S. Mercurio, E. Tolosano, Heme in pathophysiology: a matter of scavenging, metabolism and trafficking across cell membranes, *Front. Pharmacol.* 5 (2014) 61.
- [23] A.P. Delaney, A. Dan, J. McCaffrey, S. Finfer, The role of albumin as a resuscitation fluid for patients with sepsis: a systematic review and meta-analysis, *Crit. Care Med.* 39 (2011) 386–391.
- [24] S. Akech, S. Gwer, R. Idro, G. Fegan, A.C. Eziefula, C.R. Newton, M. Levin, et al., Volume expansion with albumin compared to gelofusine in children with severe malaria: results of a controlled trial, *PLoS Clin Trials* 1 (2006) e21.
- [25] K. Maitland, A. Pamba, M. English, N. Peshu, K. Marsh, C. Newton, M. Levin, Randomized trial of volume expansion with albumin or saline in children with severe malaria: preliminary evidence of albumin benefit, *Clin. Infect. Dis.* 40 (2005) 538–545.
- [26] E. Karnaukhova, S.S. Krupnikova, M. Rajabi, A.I. Alayash, Heme binding to human alpha-1 proteinase inhibitor, *Biochim. Biophys. Acta* 1820 (2012) 2020–2029.
- [27] S. Janciauskiene, S. Tumpara, M. Wiese, S. Wrenger, V. Vijayan, F. Gueler, R. Chen, et al., Alpha-1-antitrypsin binds heme and prevents oxidative activation of human neutrophils: putative pathophysiological significance, *J. Leukoc. Biol.* 102 (2017) 1127–1141.
- [28] F.A. Wagener, A. Eggert, O.C. Boerman, W.J. Oyen, A. Verhofstad, N.G. Abraham, G. Adema, et al., Heme is a potent inducer of inflammation in mice and is counteracted by heme oxygenase, *Blood* 98 (2001) 1802–1811.
- [29] E. Zilian, H. Saragih, V. Vijayan, O. Hiller, C. Figueiredo, A. Aljabri, R. Blasczyk, et al., Heme oxygenase-1 inhibits HLA class I antibody-dependent endothelial cell activation, *PLoS One* 10 (2015), e0145306.
- [30] S. Singla, J.R. Sysol, B. Dille, N. Jones, J. Chen, R.F. Machado, Hemin causes lung microvascular endothelial barrier dysfunction by necroptotic cell death, *Am. J. Respir. Cell Mol. Biol.* 57 (2017) 307–314.
- [31] F. Vinchi, L. De Franceschi, A. Ghigo, T. Townes, J. Cimino, L. Silengo, E. Hirsch, et al., Hemopexin therapy improves cardiovascular function by preventing heme-induced endothelial toxicity in mouse models of hemolytic diseases, *Circulation* 127 (2013) 1317–1329.
- [32] V. Vijayan, F. Wagener, S. Immenschuh, The macrophage heme-heme oxygenase-1 system and its role in inflammation, *Biochem. Pharmacol.* 153 (2018) 159–167.
- [33] S. Chen, X. Lv, B. Hu, L. Zhao, S. Li, Z. Li, X. Qing, et al., Critical contribution of RIPK1 mediated mitochondrial dysfunction and oxidative stress to compression-induced rat nucleus pulposus cells necroptosis and apoptosis, *Apoptosis* 23 (2018) 299–313.
- [34] K.M. Robinson, M.S. Janes, M. Pehar, J.S. Monette, M.F. Ross, T.M. Hagen, M. P. Murphy, et al., Selective fluorescent imaging of superoxide in vivo using ethidium-based probes, *Proc. Natl. Acad. Sci. U.S.A.* 103 (2006) 15038–15043.
- [35] S. Shetty, R. Kumar, S. Bharati, Mito-TEMPO, a mitochondria-targeted antioxidant, prevents N-nitrosodiethylamine-induced hepatocarcinogenesis in mice, *Free Radic. Biol. Med.* 136 (2019) 76–86.
- [36] S. Sohrab, D.N. Petrusca, A.D. Lockett, K.S. Schweitzer, N.I. Rush, Y. Gu, K. Kamocki, et al., Mechanism of alpha-1 antitrypsin endocytosis by lung endothelium, *Faseb. J.* 23 (2009) 3149–3158.
- [37] C.J. Folts, N. Scott-Hewitt, C. Proschel, M. Mayer-Proschel, M. Noble, Lysosomal Re-acidification prevents lysophospholipid-induced lysosomal impairment and cellular toxicity, *PLoS Biol.* 14 (2016), e1002583.
- [38] C.M. Deus, K.F. Yambire, P.J. Oliveira, N. Raimundo, Mitochondria-lysosome crosstalk: from physiology to neurodegeneration, *Trends Mol. Med.* 26 (2020) 71–88.
- [39] S. Petrillo, D. Chiabrando, T. Genova, V. Fiorito, G. Ingoglia, F. Vinchi, F. Mussano, et al., Heme accumulation in endothelial cells impairs angiogenesis by triggering paraptosis, *Cell Death Differ.* 25 (2018) 573–588.
- [40] A.L. True, M. Olive, M. Boehm, H. San, R.J. Westrick, N. Raghavachari, X. Xu, et al., Heme oxygenase-1 deficiency accelerates formation of arterial thrombosis through oxidative damage to the endothelium, which is rescued by inhaled carbon monoxide, *Circ. Res.* 101 (2007) 893–901.
- [41] S. Sohrab, D.N. Petrusca, A.D. Lockett, K.S. Schweitzer, N.I. Rush, Y. Gu, K. Kamocki, et al., Mechanism of alpha-1 antitrypsin endocytosis by lung endothelium, *Faseb. J.* 23 (2009) 3149–3158.
- [42] K.A. Serban, I. Petrache, Alpha-1 antitrypsin and lung cell apoptosis, *Ann. Am. Thorac. Soc.* 13 (Suppl 2) (2016) S146–S149.
- [43] R. Pascua-Maestro, S. Diez-Hermano, C. Lillo, M.D. Ganfornina, D. Sanchez, Protecting cells by protecting their vulnerable lysosomes: identification of a new mechanism for preserving lysosomal functional integrity upon oxidative stress, *PLoS Genet.* 13 (2017), e1006603.
- [44] C. Loov, C.H. Mitchell, M. Simonsson, A. Erlandsson, Slow degradation in phagocytic astrocytes can be enhanced by lysosomal acidification, *Glia* 63 (2015) 1997–2009.
- [45] E. Gabande-Rodríguez, A. Perez-Canamas, B. Soto-Huelin, D.N. Mitroi, S. Sanchez-Redondo, E. Martinez-Saez, C. Venero, et al., Lipid-induced lysosomal damage after demyelination corrupts microglia protective function in lysosomal storage disorders, *EMBO J.* 38 (2019).
- [46] K. Cadwell, Crosstalk between autophagy and inflammatory signalling pathways: balancing defence and homeostasis, *Nat. Rev. Immunol.* 16 (2016) 661–675.
- [47] A. Bian, M. Shi, B. Flores, N. Gillings, P. Li, S.X. Yan, B. Levine, et al., Downregulation of autophagy is associated with severe ischemia-reperfusion-induced acute kidney injury in overexpressing C-reactive protein mice, *PLoS One* 12 (2017), e0181848.
- [48] D.J. Klionsky, F.C. Abdalla, H. Abeliovich, R.T. Abraham, A. Acevedo-Aroza, K. Adeli, L. Agholme, et al., Guidelines for the use and interpretation of assays for monitoring autophagy, *Autophagy* 8 (2012) 445–544.
- [49] A. Gyongyosi, K. Szoke, F. Fenyvesi, Z. Fejes, I.B. Debreceni, B. Nagy Jr., A. Tosaki, et al., Inhibited autophagy may contribute to heme toxicity in cardiomyoblast cells, *Biochem. Biophys. Res. Commun.* 511 (2019) 732–738.
- [50] A.N. Higdon, G.A. Benavides, B.K. Chacko, X. Ouyang, M.S. Johnson, A. Landar, J. Zhang, et al., Hemin causes mitochondrial dysfunction in endothelial cells through promoting lipid peroxidation: the protective role of autophagy, *Am. J. Physiol. Heart Circ. Physiol.* 302 (2012) H1394–H1409.
- [51] Z. Gouveia, A.R. Carlos, X. Yuan, F. Aires-da-Silva, R. Stocker, G.J. Maghazal, S. S. Leal, et al., Characterization of plasma labile heme in hemolytic conditions, *FEBS J.* 284 (2017) 3278–3301.
- [52] M.G. Shapira, B. Khalfin, E.C. Lewis, A.H. Parola, I. Nathan, Regulation of autophagy by alpha1-antitrypsin: "a foe of a foe is a friend", *Mol. Med.* 20 (2014) 417–426.
- [53] X. Bai, A. Bai, J.R. Honda, C. Eichstaedt, A. Musheyev, Z. Feng, G. Huijt, et al., Alpha-1-Antitrypsin enhances primary human macrophage immunity against nontuberculous mycobacteria, *Front. Immunol.* 10 (2019) 1417.
- [54] S.M. Janciauskiene, R. Bals, R. Koczulla, C. Vogelmeier, T. Kohnlein, T. Welte, The discovery of alpha1-antitrypsin and its role in health and disease, *Respir. Med.* 105 (2011) 1129–1139.
- [55] I. Petrache, I. Fijalkowska, T.R. Medler, J. Skirball, P. Cruz, L. Zhen, H.I. Petrache, et al., alpha-1 antitrypsin inhibits caspase-3 activity, preventing lung endothelial cell apoptosis, *Am. J. Pathol.* 169 (2006) 1155–1166.
- [56] K.H. Jeong, J.H. Lim, K.H. Lee, M.J. Kim, H.Y. Jung, J.Y. Choi, J.H. Cho, et al., Protective effect of alpha 1-antitrypsin on renal ischemia-reperfusion injury, *Transplant. Proc.* 51 (2019) 2814–2822.
- [57] V. Vijayan, P. Pradhan, L. Braud, H.R. Fuchs, F. Gueler, R. Motterlini, R. Foresti, et al., Human and murine macrophages exhibit differential metabolic responses to lipopolysaccharide - a divergent role for glycolysis, *Redox Biol* 22 (2019) 101147.
- [58] V. Vijayan, T. Srinu, S. Karnati, V. Garikapati, M. Linke, L. Kamalyan, S.R. Mali, et al., A new immunomodulatory role for peroxisomes in macrophages activated by the TLR4 ligand lipopolysaccharide, *J. Immunol.* 198 (2017) 2414–2425.
- [59] H. Atamna, M. Brahmabhatt, W. Atamna, G.A. Shanower, J.M. Dhabbi, ApoHRP-based assay to measure intracellular regulatory heme, *Metall* 7 (2015) 309–321.
- [60] A. Aljabri, V. Vijayan, M. Stankov, C. Nikolin, C. Figueiredo, R. Blasczyk, J. U. Becker, et al., HLA class II antibodies induce necrotic cell death in human endothelial cells via a lysosomal membrane permeabilization-mediated pathway, *Cell Death Dis.* 10 (2019) 235.